International Journal on Electrical Engineering and Informatics - Volume 16, Number 1, March 2024

Optimal Electromagnetic Parameters of SPMSM for Electric Vehicles Based on Genetic Algorithm Technique

Trinh Cong Truong[1], Thanh Nguyen Vu[1], Nam Le Hai[1], Thang Nguyen Duy[1], Duong Doan Le Quy[1], Vuong Dang Quoc[1], Duc-Quang Nguyen[2] and Bao Doan Thanh[3,*]

[1]School of Electrical and Electronic Engineering, Hanoi University of Science and Technology
No 1, Dai Co Viet street, Hai Ba Trung District, Hanoi, Viet Nam.
[2]Faculty of Electrical Engineering, Electric Power University, Hanoi, Vietnam.
[3]Faculty of Engineering and Technology, University of Quy Nhon, Quy Nhon City, Binh Dinh,Vietnam.
*corresponding author: doanthanhbao@qnu.edu.vn

Abstract: In order to achieve the stringent performance objectives of low vibration, high power density, and efficiency, an effective design optimization of electric machines plays an important role in the field of electric vehicles and industries. Conventional optimization methods sometimes suffer from long computation times or are unable to reach a global solution. Firstly, an analytical model is introduced to define required parameters of the proposed motor. Then a novel technique based on the GAs is proposed to optimize the electromagnetic parameters of the surface-mounted permanent magnet synchronous motor (SPMSM), such as reduction of the cost and total losses, improvement of performence of torque, cogging torque, torque ripple, magnetic flux and effeciency. The results before and after optimization are compared together to verify the development method.

Keywords: Surface-mounted permanent magnet synchronous motor (SPMSM), genetic algorithms (GAs), electromagnetic torque, cogging torque, analytical model, Electric Vehicles.

1. Introduction

The permanent magnet synchronous motors (PMSMs) find extensive application in several industries, including robotics, electric vehicles and industrial automation. Because of their effectiveness, small size, and responsiveness to control signals, they are a well-liked option for applications needing both high precision and energy efficiency [1]–[6]. All things considered, PMSMS have made a substantial contribution to the advancement of numerous technologies as well as the creation of more ecologically and energy-efficient systems neodymium-iron-boron (NdFeB) and samarium-cobalt (SmCo) [7].

The fractional-slot concentrated winding is frequently used for high-torque applications. When there are fewer than one and non-integer slots per pole each phase, the winding configuration is referred to as a fractional-slot winding. It is called a focused winding when every coil in the winding is looped around every stator teeth. This kind of winding makes the motor very beneficial for low-speed direct drive transmission systems because of its low copper loss, high slot fill factor, low end turn length, and high efficiency. In contrast to integral slot machines, fractional-slot systems have certain disadvantages, such as a somewhat lower winding factor and a larger harmonic content in the magnetomotive force (MMF) distribution [8]-[11]. As a result, depending on the planned uses of the motor, the number of pole pairs and slots must be appropriately combined in the design.

One popular search heuristic for producing efficient solutions to optimization and search issues is the genetic algorithm (GA). The GA uses strategies including inheritance, mutation, selection, and crossover—all of which are influenced by natural evolution—to produce answers for optimization issues. Because of its adaptability, it is an effective tool for big dataset analysis and worldwide optimization [12]. This technique has been used by many researchers to investigate and analysize the best designs for PMSMs [13]–[24].

In reference [13], this work developed a multi-objective optimization design method for the PMSM based on the artificial bee colony algorithm, which aims to achieve high dynamic

Received: September 4th, 2023. Accepted: March 30th, 2024
DOI: 10.15676/ijeei.2024.16.1.9

performance and high efficiency of PMSMs. The mechanical and electrical time constants were the first important characteristics to be determined analytically using the PMSM's magnetic field analytical model. The second set of optimization objectives was the efficiency as well as the mechanical and electrical time constants. Third, using a finite-element analysis, the efficiency and dynamic performance of the original motor and the optimized motor were compared. In reference [14], the authors combined the sudomain model with the GA technique to perform an optimal design of SPMSM. In this paper, the subdomain model was first established to accurately assess the flux density harmonics. Subsequently, the pareto optimal set of solutions was searched for using the GA with the time-saving subdomain model. Lastly, to validate the new design motor's electromagnetic performance, a finite elment method (FEM) was used to compare the new design's performance to both the original and traditional GA optimum designs. In reference [15], this work proposed the optimization design of a SPMSM using Gas and the Taguchi method. In order to maximize the motor efficiency, the GAs were employed along with the Taguchi optimization method and FEM to calculate the motor performance, which was produced by the Taguchi design of tests. In reference [16]-[18], the paper proposed the best design for a SPMSM to reduce torque pulsations and saves magnet costs. The suggested SPMSM is designed with two-grade bonded NdFeB and one-grade ferrite magnets, based on a conventional SPMSM with single-grade bonded NdFeB magnets. It was then optimized by combining the Kriging method with a genetic algorithm, in order to further minimize torque pulsations and save the cost of the magnets by maintaining the high average torque. Consequently, the improved SPMSM exhibited significantly lower cogging torque, torque ripple, and magnet cost in comparison to the standard SPM motor. In reference [19], an enhanced adaptive genetic algorithm was introduced for the PMSM design optimization. In this study, the iterative duration and streamline the magnetic circuit computation throughout the optimization process were effectively decreased. In reference [20], A multi-objective optimal design method for the SPMSM was presented to maximize efficiency while lowering material costs. In this study, the GA was also applied to carry out the optimization. Furthermore, a finite element approach was suggested to verify an extensive evaluation and contrast of the deviations between the original and ideal designs.

In this study, a combination of analytical model and GA technique is proposed to optimize electromagnetic parameters of SPMSM. Firstly, an analytical model is introduced to define required parameters of the proposed motor. Then a novel technique based on the GAs is proposed to optimize the cost, torque, cogging torque, torque ripple, magnetic flux and effeciency. The results before and after optimization are compared together to verify the proposed technique.

2. Analytical design for SPMSM

The volume of motor can be defined based on the torque density (TRV) or based on the cooling method/system of motor (V_0), or based on the PM stress (σ_m). In general, in this context, the volume of motor is computed according to the TRV, i.e. [21]:

$$T = \frac{\pi}{4}.D_{is}^2 L.TRV, \tag{1}$$

where T is the electromagentic torque, D_{is} is the inner diameter of the stator and L is the effective length of the stator. It should be noted that the value of TRV is from 35 kNm/m^3 to 85 kNm/m^3 [18], [21].

The magnetic field density (B_g) in the air gap due to the PM is an essential part of the SPMSM. The NdFeB N35 magnet is selected for the proposed motor. It can be defined via the below expression:

$$B_g = \frac{4}{\pi} sin\left(\frac{\rho_{pm}}{2}\right) B_m, \tag{2}$$

where B_m is the flux density of the PM and ρ_{pm} is the electrical angle of the PM.

The thickness of PM (h_m) is then calculated as:

$$h_m = \frac{\mu_r g B_g \pi}{B_r.4sin\left(\frac{\rho pm}{2}\right) - B_g \pi}, \quad (3)$$

where B_r is the PM remanence, μ_r is the relative permeability of the PM and and g is the length of air gap.

3. Optimization Technique

The SPMSM optimization is a multi-objective problem with a lot of variables and restrictions. The variables chosen are crucial since they have an immediate effect on the output results. The variables (from z1 to z_7) are used to optimize the proposed motor as follows:

- z_1 is the inner stator diameter
- z_2 is air gap length;
- z_3 is height of the stator yoke;
- z_4 is the height of the rotor yoke;
- z_5 is the width of the tooth;
- z_6 is thecurrent density;
- z_7 is the number of turns per tooth.

Where the variables z_2, z_6, and z_7 are related to the PM size and copper loss, and z_1, z_3, z_4, and z_5 are variables related to the iron loss and steel volume. The choice of the variable values of each variable is very important in the optimal calculation process because it determines the accuracy of the built method as well as the number of iterations and time to find the convergence point of the optimal process. The correct choice of variable values has to be taken into account the impact of the parameters set in the variation of the engine configuration as well as the variation of the parameter operation of the database these changed variables. Table 1 provides the constraint boundaries of optimal variables.

Table 1. Constraint boundaries of optimal variables.

Variable	Lower boundary	Upper boundary
z_1 (mm)	145	155
z_2 (mm)	0,7	1.1
z_3 (mm)	10	15
z_4 (mm)	10	15
z_5 (mm)	12	17
z_6 (A/mm2)	4,5	5,5
z_7 (turns)	50	55

It is also necessary to define the objective functions, namely the minimization of material cost and total loss. The costs related to electrical steel, copper, and magnets are included in the material cost and are as follows:

$$C = c_{Fe}(M_s + M_r + M_t) + c_{Cu}M_{Cu} + c_m M_m \quad (4)$$

where c_{Fe}, c_{Cu}, c_m are the cost of electrical steel, copper and magnet respectively. The terms M_s, M_r, M_t and M_m are defined as [4]:

$$M_s = A_1.\frac{4A_2z_1z_3 - 4z_3^2}{z_1^2};\ M_r = A_1.\frac{4z_4(z_1 - 2A_3z_2) - 4z_4^2}{z_1^2}, \quad (5a – b)$$

$$M_t = \frac{A_1}{z_1^2}.\left\{\frac{\pi}{4}[(A_2z_1 - z_3)^2 - z_1^2] - N_s\left[(A_4z_1 + A_8 - (A_2-1)z_5 - A_6z_3)z_1 - \left(\frac{2\pi}{N_s}A_5 + z_5\frac{\pi}{N_s}z_3\right)z_3 + \frac{1}{2}h_w z_5 + A_7\right]\right\}; \quad (6)$$

$$M_{Cu} = \frac{\gamma_{Cu} I Q_s L}{z_6.10^{-6}};\ M_m = 2p\gamma_m V_m 10^{-9}. \quad (7b – c)$$

The factors from A1 to A8, and z1 to z8 are expressed as:

$$A_1 = \frac{\pi}{4}\gamma_{Fe}V_r.10^{-9};\ A_2 = \sqrt{\frac{V_s}{V_r}};\ A_3 = \frac{\mu_r B_m}{B_r - B_m} + 1;\ A_4 = (A_2 - 1)A_2\frac{\pi}{N_s};\ A_5 = h_{so} + h_w;$$

$A_6 = \frac{\pi}{N_s}(2A_2 - 1);\quad A_7 = h_{so}b_{so} + \frac{1}{2}h_w b_{so} + \frac{\pi h_w}{N_s};\qquad A_8 = \frac{1}{2}\frac{\pi h_w}{N_s} - \frac{\pi}{N_s}A_5.$

where the papermeters V_s, V_r, V_m, B_r, B_m, h_w, h_{so}, b_{so} stand for the stator, rotor, and magnet volumes, as well as the magnets operating remanence at working temperature, flux density of the magnets, wedge height, tooth tip depth, and semi-closed slot opening width. The terms γ_{fe}, γ_{Cu}, γ_m are the mass of steel, copper and PM, respectively. The term ρ_{Cu} is the rcopper esistivity, B_m is the magnetic flux of PM, B_r is the remanent PM and p is the number of pole pair.

The total losses in the SPMSM consisting of the iron, copper and additional losses are expressed as [21]:

$$P_{loss} = P_{Fe} + P_{Cu} = p_s M_s + p_r M_r + p_t M_t + N_s I^2 R \tag{8}$$

Where:
- N_s is the number of slot;
-I is the phase current;
- R is the resistance of the winding in each tooth;
-M_s is the mass of stator yoke;
-M_r is the mass of rotor yoke;
-M_t is stator teeth PM.

The loss per kilogam in stator yoke (p_s) is

$$p_s = k_h f \left(\frac{B_m V_m 10^{-6}}{2V_r(A_3-1)k_j}\right)^{1,6} \left(\frac{z_1^2}{z_2 z_3}\right)^{1,6} + k_e f^2 \left(\frac{B_m V_m 10^{-6}}{2V_r(A_3-1)k_j}\right)^2 \left(\frac{z_1^2}{z_2 z_3}\right)^2, \tag{9}$$

the loss per kilogam in rotor yoke (p_r) is

$$p_r = k_h f \left(\frac{B_m V_m 10^{-6}}{2V_r(A_3-1)k_j}\right)^{1,6} \left(\frac{z_1^2}{z_2 z_4}\right)^{1,6} + k_e f^2 \left(\frac{B_m V_m 10^{-6}}{2V_r(A_3-1)k_j}\right)^2 \left(\frac{z_1^2}{z_2 z}\right)^2, \tag{10}$$

and the loss per kilogam in stator teeth yoke (p_t) is

$$p_t = k_h f \left(\frac{p.B_m V_m 10^{-6}}{N_s V_r(A_3-1)k_j}\right)^{1,6} \left(\frac{z_1^2}{z_2 z_5}\right)^{1,6} + k_e f^2 \left(\frac{p.B_m V_m 10^{-6}}{N_s V_r(A_3-1)k_j}\right)^2 \left(\frac{z_1^2}{z_2 z_5}\right)^2. \tag{11}$$

The resistance of each ended coil in (11) is calculated as:

$$R = \frac{\rho_{Cu}.L}{\frac{I}{z_6}.10^{-6}} = \frac{\rho_{Cu}.L z_6}{I.10^{-6}}, \tag{12}$$

where the length of each teeth is defined:

$$L = 2z_7\left\{z_5 + \frac{V_r}{z_1^2} + \frac{A_9}{\sqrt{z_6}}ceil\left[\frac{z_7}{floor\left[\left(\frac{\pi}{N_s}z_1 - \frac{2\pi}{N_s}A_5 - z_5\right)\frac{\sqrt{z_6}}{A_9}\right]}\right]\right\};\ A_9 = 1,095\sqrt{\frac{4I}{\pi}} \tag{13}$$

4. Numerical and optimal results

The test problem is a practical SPMSM given in Table 2:

Table 2. Main parameters of SPMSM.

Parameter	Value	Unit
Rated Power	7500	W
Terminal voltage	500	V
Number of slot	12	Slot
Number of pole pairs	4	Plole
Frequency	50	Hz

The distribution of flux density (*B*) in the stator and rotor before optimization (*left*) and after optimization (*right*) is pointed out in Figure 1.

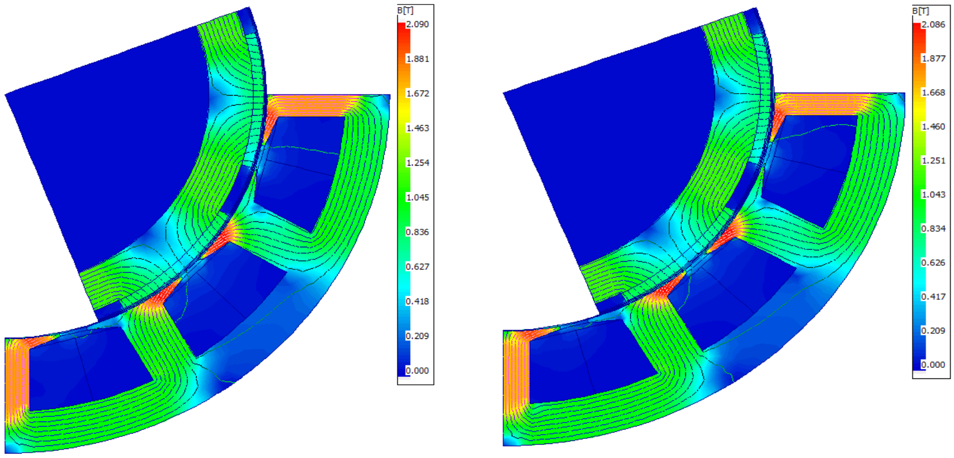

Figure 2. Flux density distribution on the stator and rotor before optimization (*left*) and after optimization (*right*).

It can be seen that, before optimization, the maximum value of flux density is 2.09T at the tooth tip position. After optimization, the maximum value of flux density is 2.086T at the same position. This means that the maximum flux density value on the air gap decreases by 0.004T. This value is very small and insignificant, so it can be neglected. The distribution of flux density at the air gap before and after optimization remains almost unchanged, with only insignificant differences in the amplitude of flux density at some positions due to changes in the amplitude of high-order harmonic waves. The distribution of flux density after optimization and the amplitude of harmonic waves of flux density at the air gap are shown in Figure 3. The distribution of cogging torque for two different cases (the before and after optimizations) is shown in Figure 4. The value after optimization is smaller than that before optimization. This result is consistent with the intended reduction of cogging torque. The back EMF distribution is shown in Figure 5. It can be observed that before optimization, the value of the back EMF is 300.4V rms, after optimization it is 299.2V rms, a decrease of 1.2V. However, both of these values are still lower than the supply voltage (353.6V rms). The reduction in the value of back EMF is because after optimization, the total harmonic distortion (TDH) value of the back EMF waveform decreases from 7.2% to 5.4% due to a significant decrease in the amplitude of the 5^{th}, 11^{th}, and 13^{th} order harmonic waves, resulting in a decrease in the total value of back EMF. This is the desired outcome as after optimization, the back EMF waveform becomes more sinusoidal, indicating better torque quality. The amplitude of harmonic waves of the back EMF is also depicted in Figure 6. Thanks to the decrease in the amplitude of some high-order harmonic waves, the losses caused by these harmonics also decrease. Consequently, this increases the efficiency of the machine from 93.8% before optimization to 94% after optimization.

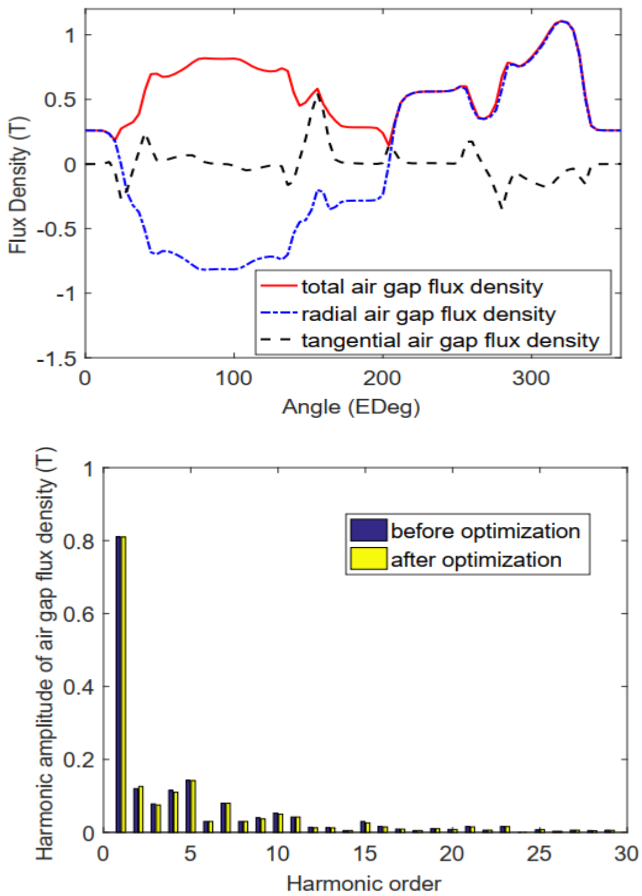

Figure 3. Flux density with different components (*top*) and harmonic amplitude of air gap flux density (*bottom*).

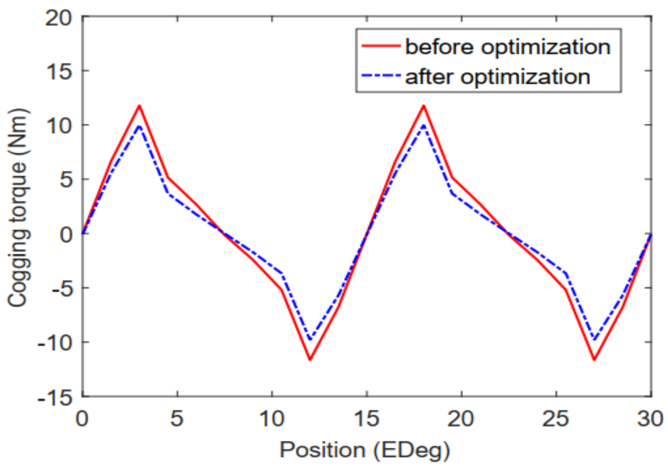

Figure 4. Distribution of cogging torque.

The torque characteristic is prensted in Figure 7. It should be noted that the torque at the motor shaft is also increased after optimization, from 95.8 Nm to 96.2 Nm. As mentioned earlier, due to the decrease in THD of the back EMF waveform, along with the reduction in cogging torque, the torque ripple of the motor decreases from 10.25% to 7.9%. The torque ripple and cogging torque are shown in the figure below. With such small torque ripple values, additional techniques such as drilling holes in the rotor core or using skewed magnets can further flatten the torque waveform, maximizing the output torque quality of the motor. Thus, after the optimization process, both power, efficiency, and torque at the motor shaft are increased. The values of torque ripple and THD of the back EMF waveform are significantly reduced. These are all expected results, demonstrating the validity of the optimization method developed in this study.

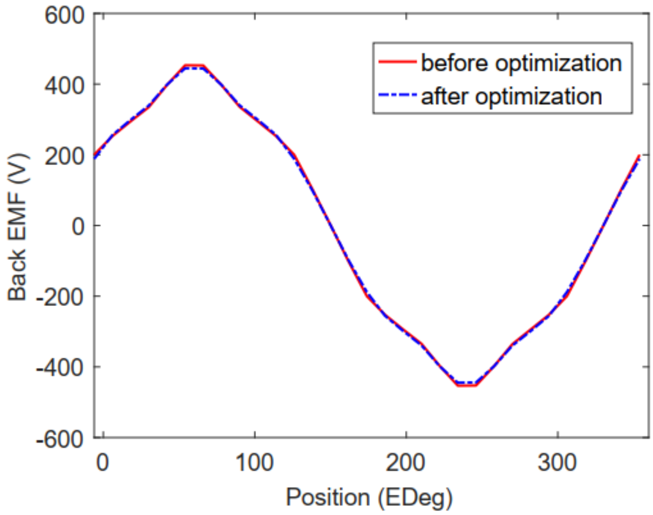

Figure 5. Distribution of the back EMF.

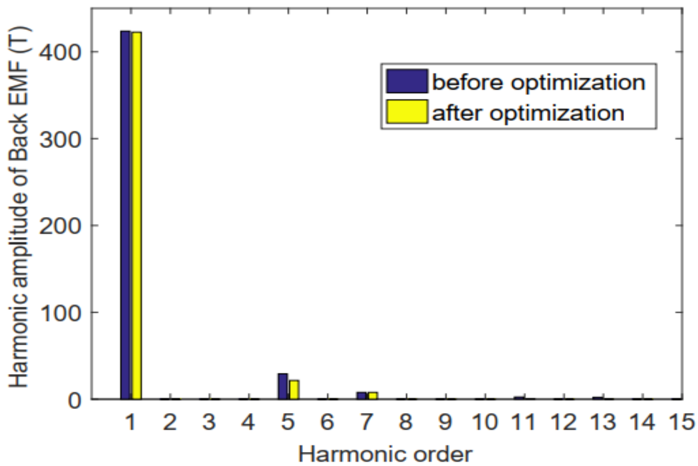

Figure 6. Harmonic amplitude of of the back EMF.

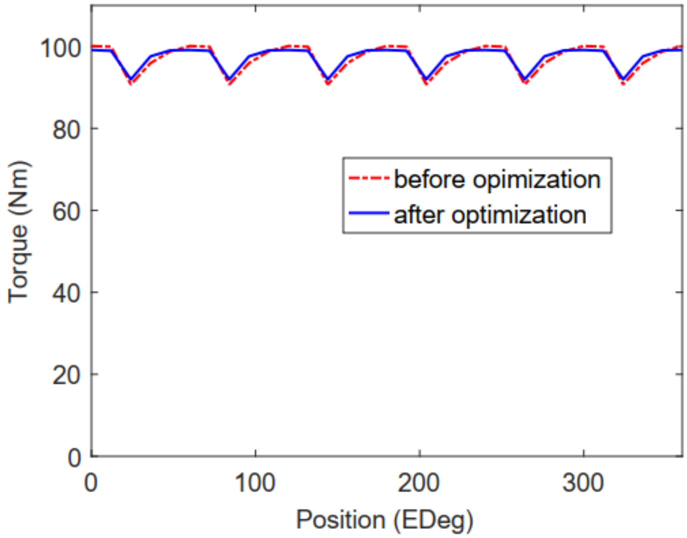

Figure 7. Distribution of the torque.

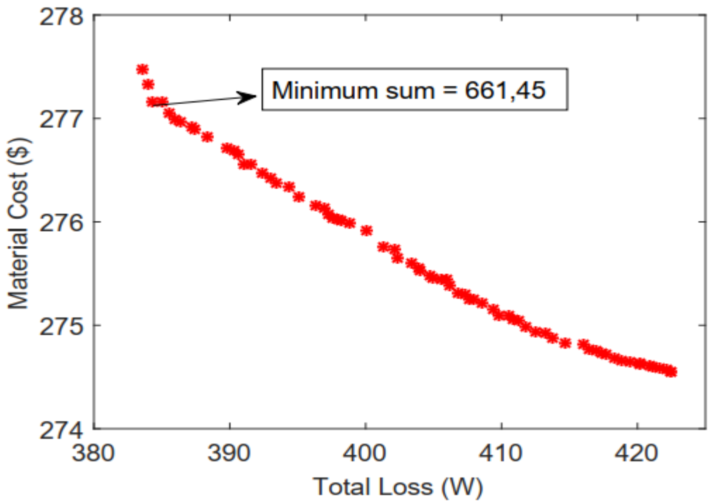

Figure 8. Pareto front results.

Pareto front results is shown in Figure 8. It can be observed that the two objective functions, material cost and total losses, exhibit an inverse relationship: as the material cost decreases, the losses increase, and vice versa, as the losses decrease, the material cost increases. In this paper, the authors chose the point of minimum value for the sum of both objective functions to perform the calculation process for the motor parameters after optimization. The optimization results on main parameters of the SPMSM is given in Table 2. The optimization process produced favorable results. The torque ripple percentage reduced by 2.35%, dropping from 10.25% to 7.9%. Moreover, the motor's efficiency increased from 93.8% to 94%. The power factor remained relatively consistent, while the back EMF decreased from 7,2% to 5,4%. Furthermore, the torque output exhibits smoother performance post-optimization, signaling a decrease in torque ripple. Despite a slight rise in flux density on the tooth, it does not adversely impact any motor parameters during operation. These favorable outcomes underscore the advantageous comparison between the optimized design and the original configuration.

Table 2. Optimal results on main parameters of the SPMSM.

Parameters	**Before optimization**	**After optimization**
Stator outer diameter (mm)	222,15	224,42
Stator inner diameter (mm)	151,4	151,6
Tooth width (mm)	14	14,6
Slot height (mm)	22,5	23,2
Magnet thickness (mm)	3	3
Magnet electrical angle	130	131
Active length of iron core (mm)	151,4	151
Number of turns	50	50
Conductor diameter (mm)	1,96	1,97
Output power (W)	7531,6	7552,5
Back EMF (V)	173,5	172,8
Efficiency (%)	93,8	94
Torque Ripple (%)	10,25	7,9
Power factor	0,94	0.94
Shaft torque (Nm)	95,8	96,2
Back EMF THD (%)	7,2	5,4

5. Conclusion

This study focuses on designing an SPMSM with a genetic algorithm integrated into a multi-objective optimization strategy. A fractional-slot focused winding 7.5 kW SPMSM's dimensions were calculated. Minimizing overall loss and material cost—two important factors—was the primary goal of the optimization procedure. The FEM was used to assess the motor's efficiency in order to confirm the efficacy of the chosen variables and constraints in the optimization process. The acquired results show that the optimized design not only results in a large reduction in material costs when compared to the original design while retaining the intended level of efficiency, but it also brings about favorable improvements in other parameters like torque ripple and cogging torque. Additional target functions, like torque output, torque cogging, and torque ripple, may be developed and optimized in future work. To solve the optimization challenges and provide even more ideal results, further optimization techniques like particle swarm optimization, the cultural algorithm, the bee algorithm, and others can be used.

6. Acknowledgment

The authors also gratefully acknowledges Quy Nhon University, created favorable conditions for the authors to use the copyright-supported Ansys software program to compute and simulate the practical problem in this research. This software is the package belonging to ANSYS Electronics Desktop V19. R1.

7. References

[1]. L. Feng, S. Yu, F. Zhang, S. Jin and Y. Sun, "Study on performance of low-speed high-torque permanent magnet synchronous motor with dynamic eccentricity rotor," *The 2nd International Conference on Power Engineering (ICPE 2021)*, Nanning, Guangxi, China, December 09–11, 2021.

[2]. J. M. Crider and S. D. Sudhoff, "An Inner Rotor Flux-Modulated Permanent Magnet Synchronous Machine for Low-Speed High-Torque Applications," *IEEE Transactions on Energy Conversion*, Volume 30, Issue 3, September 2015.

[3]. L. Qinghua, "Analysis, Design and Control of Permanent Magnet Synchronous Motors for Wide-Speed Operation," Doctoral Thesis, Dept. Of Electrical Engineeering, National University of Singapore, 2005.
[4]. M. Sundaram, M. Anand, J. Chelladurai, P. Varunraj, S. J. Smith, S. Sharma, M. E. H. Assad and R. Alayi, "Design and FEM Analysis of High-Torque Power Density Permanent Magnet Synchronous Motor (PMSM) for Two-Wheeler E-Vehicle Applications," *International Transactions on Electrical Energy Systems*, 2022.
[5]. E. K. A. N. TUN and T. TIN, "Design of Conventional Permanent Magnet Synchronous Motor used in Electric Vehicle," *International Journal of Scientific Engineering and Technology Research*, ISSN 2319-8885, Vol.03,Issue.16, Pages 3289-3293, July 2014.
[6]. G. Liu, M. Liu, Y. Zhang, H. Wang and C. Gerada, "High-Speed Permanent Magnet Synchronous Motor Iron Loss Calculation Method Considering Multi-Physics Factors," *IEEE Transactions on Industrial Electronics*, Volume: 67, Issue: 7, July 2020.
[7]. Yuan, G. A. O., et al. "Neural Network aided PMSM multi-objective design and optimization for more-electric aircraft applications." *Chinese Journal of Aeronautics 35.10* (2022): 233-246.
[8]. W. A. Pluta, "Core loss models in electrical steel sheets with different orientation," *PRZEGLĄD ELEKTROTECHNICZNY (Electrical Review)*, ISSN 0033-2097, R. 87 No 9b, 2011.
[9]. P. Ponomarev, "Tooth-Coil Permanent Magnet Synchronous Machine Design for Special Applications," *Doctoral Thesis, Lappeenranta University of Technology*, Lappeenranta, Finland, October 2013.
[10]. U.-J. Seo, Y.-D. Chun, J.-H. Choi, S.-U. Chung, P.-W. Han and D.-H. Koo, "General Characteristic of Fractional Slot Double Layer Concentrated Winding Synchronous Machine," *Journal of Electrical Engineering and Technology*, March 2013.
[11]. H. Jussila, P. Salminen, M. Niemelä and J.Pyrhönen, "Guidelines for Designing Concentrated Winding Fractional Slot Permanent Magnet Machines," *2007 International Conference on Power Engineering, Energy and Electrical Drives*, 12-14 April 2007.
[12]. S. Mishra, S. Sahoo and M. Das, "Genetic Algorithm: An Efficient Tool for Global Optimization," *Advances in Computational Sciences and Technology*, ISSN 0973-6107 Volume 10, Number 8 (2017) pp. 2201-2211, 2017.
[13]. G. Cvetkovski and L. Petkovska, "Multi-objective Optimal Design of Permanent Magnet Synchronous Motor," *2016 IEEE International Power Electronics and Motion Control Conference (PEMC)*, Varna, Bulgaria.
[14]. J. Gao, L. Dai and W. Zhang, "Improved genetic optimization algorithm with subdomain model for multi-objective optimal design of SPMSM," *CES Transactions on Electrical Machines and Systems*, Volume: 2, Issue: 1, March 2018.
[15]. C.-C. Hwang, L.-Y. L, C.-T. L and Ping-Lun, "Optimal Design of an SPM Motor Using Genetic Algorithms and Taguchi Method," *IEEE Transactions On Magnetics*, Vol. 44, No. 11, November 2008.
[16]. W. Zhao, H. Shen, W. Chai, X. Wang and a. B.-i. Kwon, "Optimal Design and Experimental Test of a SPM Motor With Cost-Effective Magnet Utilization to Suppress Torque Pulsations," *IEEE Transactions On Magnetics,* 2018.
[17]. S. Mendaci, H. Allag and a. M. R. Mekideche, "Multi-Objective Optimal Design of Surface-Mounted Permanent Magnet Motor Using NSGA-II," *ACES JOURNAL,* vol. 30, no. 5, May 2015.
[18]. H. Liu, "Design of High-Efficiency Rare-Earth Permanent Magnet Synchronous Motor and Drive System," Doctoral Thesis, University of Central Florida, 2015.
[19]. Z. Haifeng, D. Zhi and Z. Jinghua, "Optimization Design and Analysis of Permanent magnet synchronous motor based on VC," *International Conference on Electrical Machines and Systems (ICEMS)*, 2017.

[20]. Truong, T.C., Vu, T.N., Duc, H.B., Quoc, V.D. (2023). Using genetic algorithms for optimal electromagnetic parameters of SPM synchronous motors. *Journal Européen des Systèmes Automatisés*, Vol. 56, No. 6, pp. 899-906. https://doi.org/10.18280/jesa.560601.

[21]. S. Zhu, W. Chen, M. Xie, C. Liu and a. K. Wang, "Electromagnetic Performance Comparison of Multi-Layered Electromagnetic Performance Comparison of Multi-Layered," in *IEEE Transactions On Magnetics*, (2020).

Trinh Cong Truong received the Engineer degree in 2021 from the Department of Electrical Engineering, School of Electrical Engineering, Hanoi University of Science and Technology. He is currently working as a master student at the Department of Electrical Engineering, Hanoi University of Science and Technology. He can be contacted at
email: trinh.congtruong@hust.edu.vn

Thanh Nguyen Vu received his PhD degree in 2015 from the Department of Electrical Engineering, School of Electrical Engineering, Hanoi University of Science and Technology. He is currently working as a head of Department of Electrical Engineering. He can be contacted at
email: thanh.nguyenvu@hust.edu.vn

Nam Le Hai is currently a third year student at the Department of Elecctrical Engineering, School of Electrical and Electronic Engineering, Hanoi University of Science and Technology. He can be contacted at
email: nam.lh210629@sis.hust.edu.vn

Thang Nguyen Duy is currently a third year student at the Department of Elecctrical Engineering, School of Electrical and Electronic Engineering, Hanoi University of Science and Technology. He can be contacted at email: thang.nd210779@sis.hust.edu.vn

Duong Doan Le Quy is currently a third year student at the Department of Elecctrical Engineering, School of Electrical and Electronic Engineering, Hanoi University of Science and Technology. He can be contacted at email: duong.dlq212493@sis.hust.edu.vn

Dang Quoc Vuong received his PhD degree in 2013 from the Faculty of Applied Sciences at the University of Liège in Belgium. He became an associate professor in 2020. He is currently working as a deputy director of Training Center of Electrical and Electronic Engineering, School of Electrical and Electronic Engineering, Hanoi, University of Science and Technology. He can be contacted at email:vuong.dangquoc@hust.edu.vn

Duc-Quang Nguyen received his PhD degree in 2013 from the Ecole Nationale Superieure d'Arts et Metiers Paristech, France. He is currently working as a lecturer at the Faculty of Electrical Engineering, Electrical Power University. His research domain encompasses modeling of electromagnetic systems and electrical machines. He can be contacted at email: quangndhtd@epu.edu.vn

Bao Doan Thanh received the B.S. degree in Electrical engineering from Ha Noi University of Science and Technology, Vietnam, in 2006, the M.S. degree from Hanoi University of Science and Technology, Vietnam, in 2010 and the Ph.D. degree from Hanoi University of Science and Technology, in 2016. He is currently working as a lecturer at Faculty of Engineering and Technology, Quy Nhon University, Vietnam. He can be contacted at email: doanthanhbao@qnu.edu.vn.